

due to this complex. In the present study this was accomplished by thorough electrochemical or chemical reduction to obtain pure solutions of the $[\text{V}(3,5\text{-di-}i\text{-tert-butylcatecholate})_3]^{2-}$ ion. It should be noted that the extinction coefficient reported by Sawyer et al. is less than half of the correct value for $[\text{V}(3,5\text{-di-}i\text{-tert-butylcatecholate})_3]$; this indicates the extent of oxidation of the V(IV) starting material and implies that over half of the vanadium remained in the tetravalent state to give rise to the EPR spectrum ($g = 1.98$, $A = 107.8$ G) observed by Sawyer et al. It is likely that this EPR spectrum is due to unreacted $\text{VO}(\text{acac})_2$, which has $g = 1.969$ and $A = 105$ G in the same solvent. Thus the data reported by Sawyer et al.²¹ represent the optical spectrum of the V(V) complex with the EPR spectrum of a V(IV) complex. In the absence of base, $[\text{V}(3,5\text{-di-}i\text{-tert-butylcatecholate})_3]^{2-}$ does not form in MeOH (similar results are obtained for catechol); presumably $[\text{V}(3,5\text{-di-}i\text{-tert-butylcatecholate})_3]^{1-}$ does form because its higher metal ion charge leads to a higher stability constant, which permits it to displace the catechol protons without need for exogenous base.

More particularly, we have been able to identify the putative "oxygen adduct" as a vanadium(V) catechol complex. This complex is formed by reaction with NO or O₂, although not stoichiometrically in the former case; we have found that purple solutions generated by introduction of NO exhibit an EPR spectrum with two sets of hyperfine couplings ($A = 107$ and 97×10^{-4} cm⁻¹), which are characteristic of vanadyl acetylacetonate and mono(catecholate). Thus the "complicated EPR spectrum that is consistent with the patterns that have been observed for square-pyramidal geometry",²¹ which Sawyer et al. attributed to superhyperfine splitting from the nitrogen of an axially symmetric NO ligand, is in fact due to a mixture of simple vanadyl complexes.

We have not in any of our experiments observed generation of the purple V(V) complex by exposure to pure CO as reported by Sawyer et al. and suggest that the improbable observation of superimposable optical spectra for both CO and O₂ adducts is more reasonably explained by exposure to oxygen in both cases.

Some of the more puzzling aspects of the report by Sawyer et al. remain unexplained—in particular the "reversibility" of "adduct formation", which we have not been able to reproduce. However, it is clear that the observations of Sawyer et al. are not due to reversible oxygen binding by vanadium catecholate complexes.

Acknowledgment. We wish to acknowledge the support of the NIH through Grant AI 11744. S.R.C. wishes to acknowledge the donors of the Petroleum Research Fund, administered by the American Chemical Society, for partial support of this research and to thank Professor E. J. Corey and K. Bloch of this department for use of their spectrophotometers. We also thank Dr. Frederick J. Hollander for his able experimental assistance and instruction in the structure analysis. Funds for the U.C.B. Chexray facility were provided by the NSF.

Registry No. $[\text{Et}_3\text{NH}]_2[\text{V}(\text{cat})_3] \cdot \text{CH}_3\text{CN}$, 82613-78-3; $[\text{Et}_3\text{NH}][\text{V}(\text{DTBC})_3]$, 82613-80-7; $[\text{Et}_3\text{NH}]_2[\text{VO}(\text{DTBC})_2]$, 82613-82-9; $\text{K}_2[\text{VO}(\text{cat})_2] \cdot \text{EtOH} \cdot \text{H}_2\text{O}$, 82659-76-5; $\text{K}_3[\text{V}(\text{cat})_3] \cdot 1.5\text{H}_2\text{O}$, 82613-84-1; $\text{VO}(\text{acac})_2$, 3153-26-2; $\text{NH}_4[\text{VO}_3]$, 7803-55-6; $[\text{V}(\text{DTBC})_3]^{2-}$, 82613-85-2; $[\text{V}(\text{DTBC})_3]^-$, 82613-86-3; $[\text{V}(\text{cat})_3]^-$, 82613-87-4; $\text{VO}(\text{cat})$, 82598-73-0; $[\text{VO}(\text{Tironate})]^{2-}$, 82613-88-5; $\text{VO}(\text{DTBC})$, 82598-74-1; $[\text{VO}(\text{Tironate})_2]^{6-}$, 82621-18-9; $[\text{V}(\text{Tironate})_3]^{8-}$, 82613-89-6.

Supplementary Material Available: Listing of observed and calculated structure factors (60 pages). Ordering information is given on any current masthead page.

Angle-Resolved Ultraviolet Photoelectron Spectroscopic Studies of CO Binding to Three Chemically Different Surfaces of ZnO. Confirmation of Step-Binding Sites on (000 $\bar{1}$)

K. L. D'Amico, M. Trenary, N. D. Shinn, Edward I. Solomon,*¹ and F. R. McFeely*

Contribution from the Department of Chemistry, Massachusetts Institute of Technology, Cambridge, Massachusetts 02139. Received December 7, 1981

Abstract: Angle-resolved photoelectron spectroscopy (ARPES) has been performed on the ZnO(000 $\bar{1}$)-CO system. These measurements are compared with previous ARPES results on (10 $\bar{1}$ 0) and (0001) surfaces and strongly support earlier suggestions that the CO which is observed to chemisorb to this surface binds to (10 $\bar{1}$ 0) step sites which contain coordinately unsaturated zinc ions but not to the (000 $\bar{1}$) terrace sites which contain only coordinatively unsaturated oxide ions.

The adsorption of CO on ZnO is an important problem in relation to methanol synthesis.² The CO-ZnO bond is unusual because of the observation of a $\sim 70\text{-cm}^{-1}$ increase in the CO stretching frequency upon chemisorption of CO on ZnO powders.³ This is in contrast to the decrease in the stretching frequency relative to the gas-phase value of 2143 cm⁻¹, which is normally

observed upon chemisorption to metals and in organometallic complexes. In an effort to gain a detailed microscopic understanding of the nature of the CO/ZnO interaction, we have recently reported a variety of ultraviolet photoelectron spectroscopic (UV PES) studies on four chemically different surfaces of ZnO:⁴⁻⁶ (0001), which contains only coordinatively unsaturated zinc sites; (10 $\bar{1}$ 0) and (11 $\bar{2}$ 0), which contain both zinc and oxide ions with

(1) Present address: Department of Chemistry, Stanford University, Stanford, CA 94305.

(2) A. L. Waddams, "Chemicals from Petroleum", 3rd ed., Wiley, New York, 1973.

(3) (a) F. Boccuzzi, G. E. Garrone, A. Zecchina, A. Bossi, and M. Camia, *J. Catal.*, **51**, 160 (1978); (b) N. S. Hush and M. L. Williams, *J. Mol. Spectrosc.*, **50**, 349 (1974).

(4) R. R. Gay, M. H. Nodine, E. I. Solomon, V. E. Henrich, and H. J. Zeiger, *J. Am. Chem. Soc.*, **102**, 6752 (1980).

(5) M. J. Sayers, M. R. McClellan, R. R. Gay, E. I. Solomon, and F. R. McFeely, *Chem. Phys. Lett.*, **75**, 575 (1980).

(6) M. R. McClellan, M. Trenary, N. D. Shinn, M. J. Sayers, K. L. D'Amico, E. I. Solomon, and F. R. McFeely, *J. Chem. Phys.*, **74**, 4726 (1981).

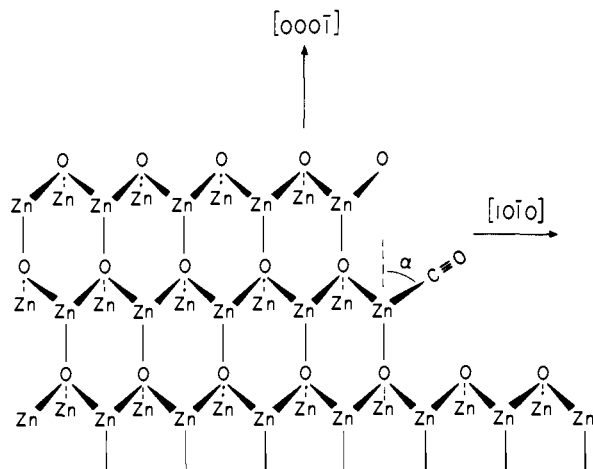


Figure 1. Structure of the ZnO (000 $\bar{1}$) surface, illustrating the double-layer step site known to exist on this surface. Such a step exposes a (10 $\bar{1}$ 0) type site onto which a CO could bind to a coordinatively unsaturated Zn ion. The Zn-C-O surface complex is oriented parallel to the [10 $\bar{1}$ 0] direction which is approximately 20° out of the plane of the paper. Due to the symmetry of the (000 $\bar{1}$) surface, this site exists in six equivalent domains.

coordinatively unsaturated positions; (000 $\bar{1}$), which nominally contains only oxide ions with open coordination positions directed normal to the surface. These studies have clearly demonstrated that CO binds carbon-end down⁴ to the coordinatively unsaturated zinc site on the (0001) and (10 $\bar{1}$ 0) surfaces, forming approximately linear Zn-C-O complexes. Here CO acts as a 5 σ donor by transferring electron density from this weakly antibonding orbital, with little π back-bonding to the CO 2 π^* orbital, resulting in a net donation of charge to the surface zinc ion. Hence the CO bond order is increased, and the CO molecule is polarized with some positive charge at the carbon. A puzzling aspect of these studies, however, was the observation⁴ of a small but nonzero amount of CO 4 σ photoelectron intensity indicative of CO bonding to the (000 $\bar{1}$) surface, which ideally contains only oxide ions. The temperature and pressure dependence of this 4 σ intensity further indicated that the CO binds with the same heat of adsorption at zero coverage to (000 $\bar{1}$) as to the other three surfaces. This led to the proposal that CO binds to zinc-containing step-defect sites on this surface. LEED studies⁷ on (000 $\bar{1}$) indicate a significant density of (10 $\bar{1}$ 0) steps, which expose zinc sites with coordinatively unsaturated positions ~70° off the surface normal (Figure 1). In this paper we present angle-resolved UV PES data that demonstrate that CO binds with an angle α of ~70° with respect to the surface normal, strongly supporting the proposal that CO binds to these step sites.

Experimental Section

The crystal used in these experiments was cut from a needle of vapor-phase-grown material and was oriented by Laue diffraction to within $\pm 1^\circ$. The surface was then polished with 1 μm Al₂O₃ and etched with dilute HCl to produce a surface free of etch pits as detectable by optical microscopy.

The surface was cleaned in situ by repeated cycles of mild (<500 eV) Ar⁺ ion bombardment, followed by repeated thermal cycling of the crystal between 700 and 80 K. This procedure was used in earlier studies on this surface, where it produced an atomically clean and well-ordered surface based on Auger and LEED analysis. The LEED pattern was indicative of surface order and a lack of reconstruction.⁴

The photoemission spectra reported here were obtained with a conventional DC discharge lamp producing He II resonance radiation ($h\nu = 40.8$ eV) which was polarized ($P \approx 0.83$) with a triple-reflection

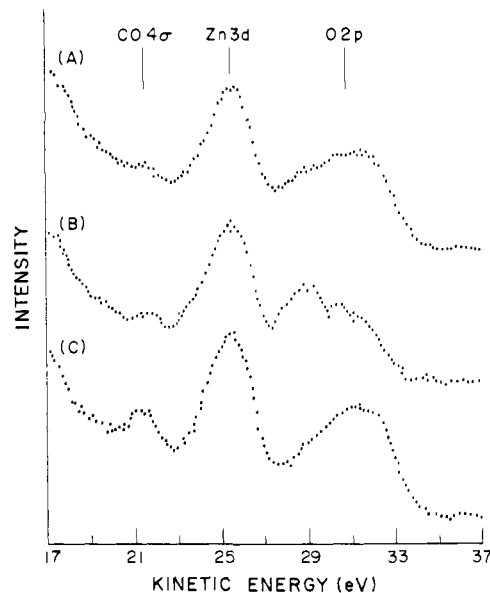


Figure 2. Angle-resolved photoelectron spectra for the ZnO (000 $\bar{1}$) surface at $T = 80$ K, with a 2×10^{-6} torr ambient of CO. The substrate Zn 3d and O 2p features and the CO 4 σ feature are indicated as follows: (A) p-polarized light, normal emission; (B) p-polarized light, detector 80° away from normal toward [1 $\bar{2}$ 10]; (C) s polarization, detector 80° away from normal toward [10 $\bar{1}$ 0].

focusing gold mirror polarizer. Photoelectrons were collected and energy analyzed by means of a two-dimensionally rotatable spectrometer of our own design.⁸

In all cases reported here, the spectra were obtained under an ambient atmosphere of 2×10^{-6} torr of CO at a surface temperature of 80 K. Many repetitions of standard collection geometries were made in the course of these experiments. This ensured that the observed angular variations in the intensity of CO-derived spectral features were due to the inherent angular distribution and not due to variations in total surface coverage. The procedure used to establish the integrity of each spectrum is the same as described earlier in our work on ZnO (0001).⁵

Results and Discussion

Three representative angle-resolved photoelectron spectra are shown in Figure 2. A clean ZnO valence-band UV PES spectrum⁴ has a feature at ~23–26 eV due to Zn 3d electrons and a feature at 29–33 eV due to O 2p electrons with some Zn 4s and 4p admixture. Upon CO chemisorption a feature at 22 eV arises due⁴ to emission from the 4 σ orbital of the adsorbed CO, while emission from the 1 π and 5 σ molecular orbitals of the CO molecule strongly overlap the zinc 3d band. Figure 2A shows the spectrum observed at normal emission (along [000 $\bar{1}$]) with p-polarized light (i.e., polarized in the plane of incidence) incident at 60° (as shown in Figure 3C). Very little 4 σ intensity is observed. However, when the detector is moved 80° toward [1 $\bar{2}$ 10], the 4 σ intensity increases substantially (Figure 2B). When the polarization is rotated to s polarization (i.e., polarized perpendicular to the plane of incidence) and the detector moved 80° toward [10 $\bar{1}$ 0], the spectrum in Figure 2C is observed. This represents the largest 4 σ intensity observed for any combination of polarization and emission angles.

This behavior is strikingly different from that exhibited by either the nonpolar (10 $\bar{1}$ 0) or the zinc-terminated (0001) surfaces.^{5,6} In both of these cases the maximum in 4 σ intensity occurs in p polarization near normal emission conditions (as in 2A). The extent of this contrast is evident from Figure 3, which compares p-polarized 4 σ angular distributions in the plane of incidence for CO adsorbed on (10 $\bar{1}$ 0), (0001), and (000 $\bar{1}$) surfaces. While the angular distributions can be strongly affected by both the molecular orientation and the orientation of the vector potential \vec{A}

(7) (a) M. Henzler, *Surf. Sci.*, **36**, 945 (1976); (b) D. Kohl, M. Henzler, and G. Heiland, *Ibid.*, **41**, 403 (1974); (c) G. Heiland, in *2nd Int. Conf. Electrophotogr.*, D. R. White, Ed., Society of Photogr. Science Engineering, Washington, D.C., 1974, p 117; (d) M. Henzler, *Appl. Phys.*, **9**, 11 (1976); (e) V. E. Henrich, H. J. Zeiger, E. I. Solomon, and R. R. Gay, *Surf. Sci.*, **74**, 682 (1978); (f) R. Nosker, P. Mark, and J. Levine, *Surf. Sci.*, **19**, 291 (1970).

(8) (a) M. J. Sayers, Ph.D. Thesis, Massachusetts Institute of Technology, Cambridge, MA, 1980; (b) M. R. McClellan, Ph.D. Thesis, Massachusetts Institute of Technology, Cambridge, MA 1981.

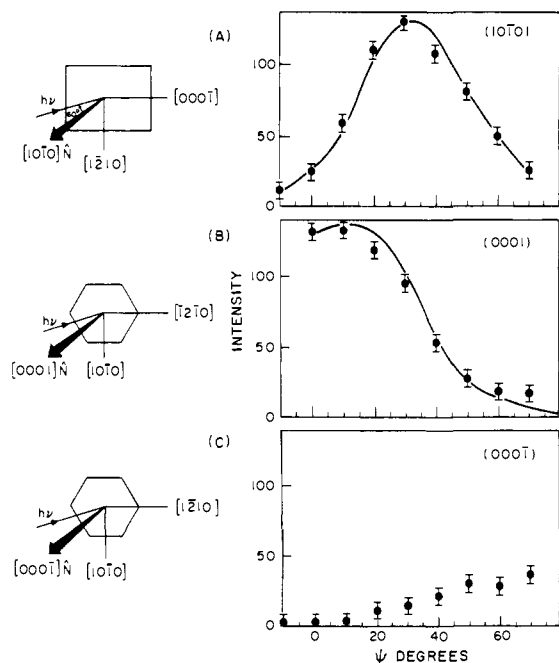


Figure 3. Photoelectron angular distributions for the CO 4σ intensity in the plane of incidence for (A) $(10\bar{1}0)$, (B) (0001) , and (C) $(000\bar{1})$ surfaces. In each case the light is incident at 60° away from the normal and in the p-polarized configuration. For all three cases, $\psi = 0^\circ$ is the surface normal, and ψ increases toward (A) $[000\bar{1}]$, (B) $[\bar{1}2\bar{1}0]$, and (C) $[\bar{1}2\bar{1}0]$.

with respect to the molecule, there is a straightforward relationship between the peak position in these particular distributions and the molecular orientations. When \bar{A} and the molecular axis are coincident, the 4σ intensity maximum is along the molecular axis.⁹

The above condition is met almost exactly for the $(10\bar{1}0)$ surface, in Figure 3A, where the molecules are directed at 30° to the surface normal in the direction of $[000\bar{1}]$.⁵ On the (0001) surface, the CO molecules stand perpendicular to the surface, and thus a coincidence of this axis and \bar{A} is impossible.⁶ The maximum is thus slightly shifted (by 10°) away from the molecular axis and toward \bar{A} (Figure 3B). In strong contrast, the intensity distribution from $(000\bar{1})$ shows no maximum but rather a continuous monotonic increase out to 80° (Figure 3C). Examination of this $(000\bar{1})$ angular distribution, along with the observation that the maximum CO 4σ intensity is obtained at an angle of 80° off normal (s polarization (Figure 2C), strongly suggests that it is the electric vector component parallel to the surface that is primarily responsible for the strong intensity at large angles. This is confirmed by the observation (not shown) that the intensity of the 4σ peak increases as the angle of incidence of the light decreases. These observations require that the angle between the adsorbed molecules and the surface normal be large and therefore suggest that the CO molecule binds at sites other than the terrace oxides for which the coordination unsaturation is normal to the surface.

In an effort to quantify further the binding geometry of CO on the $(000\bar{1})$ surface, four complete angular distributions were measured by utilizing s- and p-polarized light with both in-plane and out-of-plane sweeps. For clarity, the details of the experimental geometry for the angle-resolved experiment are shown in Figure 4.

The general detector angle is (χ, ψ) , where χ is the polar angle and is referenced to the crystal normal \bar{N} , $(000\bar{1})$, which is the \bar{Z} axis of Figure 4. ψ is the azimuthal angle. When ψ is held at 0° , varying χ from 0 to 90° corresponds to varying the detector toward $[10\bar{1}0]$. This represents the out-of-plane of incidence sweep of Figure 5A and B. When χ is held at 0° , varying ψ from 0 to 90° corresponds to varying the detector toward $[\bar{1}2\bar{1}0]$. This represents the in-plane sweep of Figure 6A and B. We note that

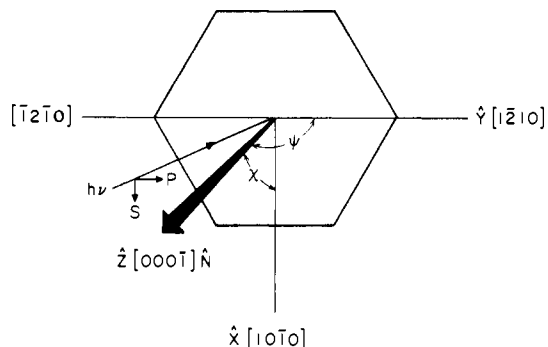


Figure 4. Coordinate system used in these experiments for defining the position of the electron detector with respect to the crystal direction. The surface normal \bar{N} is the $[000\bar{1}]$ and the \bar{Z} axis, while \bar{X} is along $[10\bar{1}0]$ and \bar{Y} is along $[\bar{1}2\bar{1}0]$. For all measurements reported here, the 40.8-eV He II photons are incident upon the crystal such that their plane of incidence contains the $[\bar{1}2\bar{1}0]$, $[000\bar{1}]$, and $[\bar{1}2\bar{1}0]$ directions, and the angle of incidence is 60° away from $[000\bar{1}]$ toward $[\bar{1}2\bar{1}0]$.

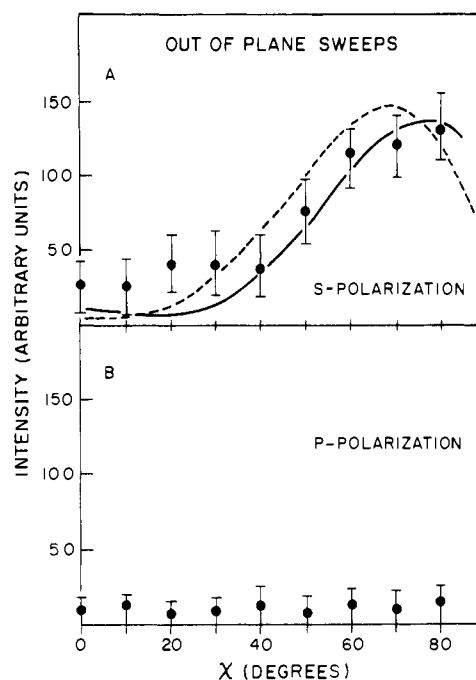


Figure 5. CO 4σ photoelectron angular distributions measured out of the plane of incidence for (A) s-polarization and (B) p-polarization conditions. The dashed and solid curves in A represent theoretical curves for a molecular orientation where the \bar{A} axis is oriented 60 and 70° , respectively, away from the surface normal toward the six symmetry-equivalent $\langle 10\bar{1}0 \rangle$ directions.

Figure 6A and B also includes the point $(0^\circ, -10^\circ)$, which corresponds to moving the detector, in the plane, 10° toward $[\bar{1}2\bar{1}0]$. In all of the above four sweeps, the photon beam is incident upon the crystal from the angle $(\chi, \psi) = (0^\circ, -60^\circ)$. Polarization in the s configuration is when \bar{A} is perpendicular to the plane of incidence, while the p configuration is for \bar{A} oriented within the plane of incidence.

The angular distributions were analyzed by using a model previously discussed in detail for the (0001) surface.⁶ This model assumes that the form of the angular distribution of the CO 4σ orbital is unchanged upon adsorption and is adequately described by space-fixed free-molecule calculations.⁹ The only role of the surface, then, is to modify the applied (partially polarized) electromagnetic field. This approximation has been repeatedly tested and has been found to yield physically reasonable and self-consistent results for the orientation of CO molecules on other ZnO surfaces,^{5,6} as well as on a variety of low- and high-index metal surfaces.¹⁰

(9) J. W. Davenport, Ph.D. Thesis, University of Pennsylvania, Philadelphia, PA, 1976.

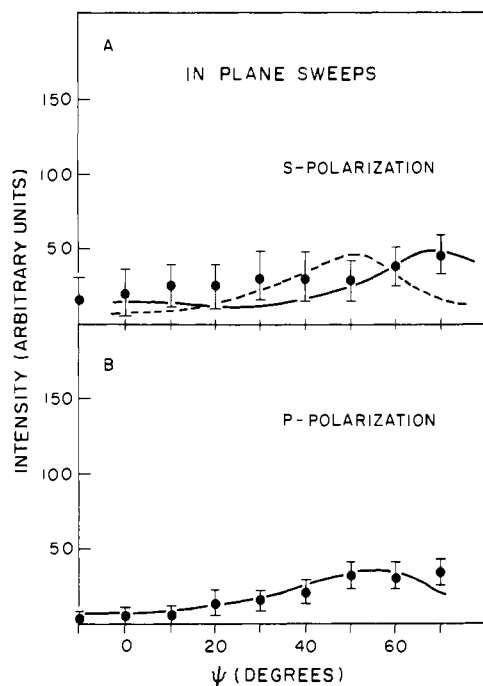


Figure 6. CO 4σ photoelectron angular distributions measured in the plane of incidence for (A) s-polarization and (B) p-polarization conditions. The dashed curve (60°) in A and the solid curve (70°) in both A and B represent theoretical plots for CO orientations as discussed for Figure 5 above.

Comparisons¹¹ of all four of the angular distributions in Figures 5 and 6 with our previous ZnO (10 $\bar{1}$ 0) and (0001) results lead to two conclusions: (1) the CO 4σ intensity is uniformly quite low throughout; (2) while the angular distributions do not show the well-defined structure of the (0001) and (10 $\bar{1}$ 0) surfaces, they do indicate an increase in intensity at angles very far from the surface normal. As an aid in interpreting the experimentally observed intensity profiles, we have included theoretical plots for molecules oriented 60 and 70° away from the surface normal where these plots are the sums of the contributions from the six symmetry-equivalent (10 $\bar{1}$ 0) directions.

Figure 5B shows the angular distributions as the detector is scanned from normal emission toward [10 $\bar{1}$ 0], obtained with p-polarized excitation. Due to the low intensities exhibited in this scan and the rapidly sloping background, (see, e.g., Figure 2A), the values obtained for the peak areas are strongly dependent upon the details of the background-subtraction procedure. The rather large error bars in this (and similar) distributions largely reflect this ambiguity. However, for the purposes of the analysis presented here, it is sufficient to characterize the emission into these angles as weak and unstructured. Due to this low 4σ intensity, we have omitted any theoretical plots from Figure 5B. The important point to realize is that for molecules bound perpendicularly to the surface, a sharp monotonic falloff of the intensity would be ex-

pected. Instead, the distribution shows uniformly low intensity and little structure.

When the polarization vector is rotated into the s configuration and the angles are rescanned, the distribution of the 4σ intensity is strikingly altered (Figure 5A). A region of background-level intensity persists from normal emission to $\sim 40^\circ$ followed by a rise to the strongest peak observed in these experiments. The dashed curve illustrates the expected intensity pattern for molecules oriented 60° away from the surface normal \bar{N} , and the solid curve illustrates the expected intensity pattern for molecules oriented 70° off the surface normal.

Figure 6B is the same plot as illustrated in Figure 3C. A smooth variation of the CO 4σ intensity is present which shows no maximum but rather increases out to 70° off the surface normal. We have included a theoretical plot for molecules oriented 70° off the surface normal. The final angular distribution is the in-plane detector sweep under s-polarization conditions, shown in Figure 6A along with theoretical plots for molecules oriented 60 and 70° away from the surface normal.

One can see that the theoretical plots of 60 and 70° in Figure 5A model the observed intensity quite well, with the 70° calculation generating a somewhat better fit. Angles of orientation smaller than 60° or larger than 70° result in the qualitative trend of shifting the predicted distribution maximum closer to normal emission or closer to [10 $\bar{1}$ 0], respectively. This trend is also exhibited in Figure 6A and holds for the other plots; however, as mentioned above, the intensity is so low that inferring a particular molecular orientation from Figures 5B and 6B is inappropriate.

It is clear from the preceding discussion that the angle between the (000 $\bar{1}$) surface normal and the CO molecular axis is quite large and that the data are best explained by a CO-ZnO angle of $\sim 70^\circ$. This would place the molecule roughly along the coordinatively unsaturated position of the Zn ion on the (10 $\bar{1}$ 0) step sites, in confirmation of our earlier proposal⁴ (Figure 1, $\alpha \approx 70^\circ$). This interpretation is quite consistent with the observation⁴ that the CO heat of adsorption on this surface is the same as on the other three low-index faces where CO has been shown to bind to the Zn terrace sites. This defect-binding geometry also explains the substantial CO 4σ intensity observed on the (000 $\bar{1}$) surface during our angle-integrated UV PES experiments⁴ because in those experiments the CO molecules were particularly well oriented with respect to the CMA cone of acceptance of photoelectrons.

In summary, the results of our angle-integrated and angle-resolved UV PES studies⁴⁻⁶ on the (10 $\bar{1}$ 0), (0001), (000 $\bar{1}$), and (11 $\bar{2}$ 0) low-index surfaces of ZnO have shown that CO consistently binds carbon-end down to the coordinatively unsaturated Zn sites and roughly along the unsaturated Zn direction. The angular behavior of the Zn-C-O surface complexes are completely consistent with the results of LEED studies⁷ where in all cases no symmetry-changing reconstructions are observed and where the polar surfaces are known to form a high density of (10 $\bar{1}$ 0) defect-step sites.¹²

Acknowledgment. This research was performed on an instrument constructed under and supported by the Joint Services Electronics Program under Contract No. DAA6-29-78-C-0020. Support for this work was provided by the Department of Energy under Grant De-A502-78ER04998. We thank Susan Cohen for useful discussions and help with final preparation of the manuscript.

Registry No. CO, 630-08-0; ZnO, 1314-13-2.

(10) (a) C. L. Allyn, T. Gustafsson, and E. W. Plummer, *Solid State Commun.*, **24**, 531 (1977); (b) C. L. Allyn, T. Gustafsson, and E. W. Plummer, *Chem. Phys. Lett.*, **47**, 127 (1977); (c) G. Apai, P. S. Wehner, R. W. Williams, J. Störr, and D. A. Shirley, *Phys. Rev. Lett.*, **37**, 1497 (1976); (d) R. J. Smith, J. Anderson, and G. J. Lapeyre, *Phys. Rev. Lett.*, **37**, 1081 (1976); (e) T. Gustafsson and E. W. Plummer, in "Photoemission and the Electronic Properties of Surfaces"; B. Feuerbacher, B. Fitton, and R. F. Willis, Eds., Wiley-Interscience, New York, 1978; (f) N. D. Shinn, M. Trenary, M. R. McClellan, and F. R. McFeely, *J. Chem. Phys.*, **75**, 3142 (1981).

(11) While it is not possible to normalize the s-polarization scans exactly to the p-polarization scans, clearly the point $(\chi, \psi) = (0^\circ, 0^\circ)$ is common to both in-plane and out-of-plane p-polarization scans, and their relative intensities can be compared. The same is true for the in-plane and out-of-plane scans for s polarization.

(12) Unfortunately, two problems arise with attempting to quantify directly the number of defect (10 $\bar{1}$ 0) step sites on the (000 $\bar{1}$) face. First, even at liquid-nitrogen temperatures, the surface sites are not saturated,⁴ and second, direct comparisons of photoelectron intensities cannot be made between the (10 $\bar{1}$ 0) and (000 $\bar{1}$) surfaces, due to the different angular anisotropies of the surfaces with respect to the electron analyzer.